Clinical Oral Investigations (2025) 29:259
https://doi.org/10.1007/s00784-025-06327-z

RESEARCH

# Biomechanical analysis of maxillary first molar intrusion using 3D printed personalized device combined with clear aligner: a finite element study and clinical application

Qin Xue[1,2] · Mei Hu[1,2] · Minglu Xu[1,2] · Xuyang Zhang[1,2] · Huaqiao Wang[3,4] · Mimi Sun[5] · Chunjuan Wang[1,3,4] · Yao He[1,3,4]

Received: 22 January 2025 / Accepted: 4 April 2025


## Abstract

**Objectives** The aim of this study is to compare the biomechanical effects of maxillary first molar intrusion using the fixed appliance, microimplant, and clear aligner with or without 3D printed personalized device, and to demonstrate the effect of this device through a relevant clinical case.

**Methods** A clinical patient with an overerupted maxillary molar was selected to construct a patient-oriented three-dimensional model of the four intrusion patterns. The initial displacement of the teeth and the stress distribution of the PDL were compared. The 3D printed personalized device was used in this case, and the data of the case was collected to assess the therapeutic effect.

**Results** The side effects of target tooth tilt and adjacent tooth displacement were obvious in fixed appliance and clear aligner, while the side effects were smaller in 3D printed personalized device, and the intrusion efficiency is slightly higher than that of microimplant. In clinical practice of 3D printed personalized device, a favorable intrusion effect was achieved.

**Conclusions** The 3D printed personalized device had relatively high intrusion efficiency and stress relaxation on the target tooth and reduced the displacement and stress concentration on the anchorage teeth to a certain extent.

**Clinical relevance** In clinical practice, clear aligner with 3D printed personalized device has a good therapeutic effect on molar intrusion.

**Keywords** 3D printed personalized device · Clear aligner · Molar intrusion · Biomechanics · Finite element analysis

✉ Chunjuan Wang
cj_wang@hospital.cqmu.edu.cn

✉ Yao He
yaohe@hospital.cqmu.edu.cn

Qin Xue
2022110493@stu.cqmu.edu.cn

Mei Hu
2023111344@stu.cqmu.edu.cn

Minglu Xu
2021110510@stu.cqmu.edu.cn

Xuyang Zhang
2021110514@stu.cqmu.edu.cn

Huaqiao Wang
wanghuaqiao@hospital.cqmu.edu.cn

Mimi Sun
495014360@qq.com

[1] The Affiliated Stomatological Hospital of Chongqing Medical University, No. 426, North Songshi Rd, Chongqing 401147, China

[2] Chongqing Key Laboratory of Oral Disease, Chongqing, China

[3] Chongqing Municipal Key Laboratory of Oral Biomedical Engineering of Higher Education, Chongqing, China

[4] Chongqing Municipal Health Commission Key Laboratory of Oral Biomedical Engineering, Chongqing, China

[5] Department of Orthodontics, Affiliated Stomatological Hospital of Chongqing Medical University, Chongqing, China

Published online: 21 April 2025

## Introduction

The prevalence of opposing tooth overeruption after posterior tooth loss due to dental caries, periodontal disease, and tooth defect ranges from 70 to 85% [1]. If the molar is missing for a long time without restoration treatment, it often causes the opposing molar to overerupt, which reduces the height of crown and causes restoration difficulties [2]. Orthodontic treatment in the opposing dentition can restore the edentulous space by changing the position of the teeth while reducing the sacrifice of tooth structure as much as possible [3].

At present, the commonly used methods to achieve molar intrusion include fixed appliance, microimplant, and clear aligner. In fixed appliance treatment, brackets and archwires are often used to achieve the intrusion of the target tooth by fabricating intrusion loops. However, the complex intraoral devices are difficult to clean, and the clinical operation is time-consuming. Microimplants were placed in the buccal and lingual side of the target tooth, and the intrusion force was achieved by the latex elastic passed on the two microimplants [4]. The advantages of microimplant are simple, comfortable, and precise intrusion force [5]. The disadvantage is that the operation is invasive, and there may be risks of implant loosening, fracture, and damage to the root of adjacent teeth [6]. Clear aligner treatment generates elastic force by the displacement between the clear aligner and the teeth, which acts on the teeth to move. The advantages are relatively invisible and aesthetic, and conducive to oral hygiene [7]. However, the efficiency of clear aligners varies greatly in different tooth movement modes [8, 9]. In the absence of occlusal contact, the effect of intrusion on overerupted molars was also reduced. With the development of digital three-dimensional (3D) printed technology, personalized printed devices have been widely used in anchorage control, assisting tooth movement and supporting orthodontic treatment processes [10–13]. The 3D printed personalized device combined with clear aligner may play a role in the intrusion of the overerupted teeth. However, its biomechanical effects are still unclear, and its clinical application methods and effects need to be explored.

Due to the limitations of in vivo studies to evaluate mechanical effects, finite element analysis (FEA) has become a common method to evaluate orthodontic biomechanics [14–16]. Three-dimensional FEA is an efficient computer simulation technology, and its basic method is to divide subjects into finite elements for calculating and analyzing [17]. FEA has the advantages of high calculation accuracy, high efficiency, low cost, and suitable for all kinds of complex shapes which now has been widely used to calculate various engineering mechanical problems [18]. FEA study can simulate clinical scenarios and has been widely used as a routine method for orthodontic mechanical analysis [19].

In this study, 3D models of fixed appliance, microimplant, clear aligner, and 3D printed personalized device combined with clear aligner were established based on a clinical case to analyze the 3D displacement and stress distribution of the periodontal ligament (PDL) of the target tooth and anchorage teeth. The application of the auxiliary device in this case was shown which provided a mechanical basis and clinical application for the use of 3D printed personalized device combined with clear aligner in the intrusion of overerupted molars.

## Materials and methods

### Data collection and model construction

A healthy patient (male, 18 years old) from the Department of Orthodontics, Affiliated Stomatological Hospital of Chongqing Medical University with an overerupted maxillary first molar and normal anatomic morphology of teeth was selected. The left maxillary first molar was defined as the intruded target tooth in this study. The dentition and maxillary bone of the patient were scanned by Cone Beam Computed Tomography (Kavo, Biberach, Germany) to obtain DICOM (Digital Imaging and Communications in Medicine) data (120 kVp; 5 mA; 0.4-mm voxel size).

The DICOM data obtained by CBCT scanning was imported into the Mimics system (version 17.0; Materialize, Belgium). A preliminary 3D model of the maxilla and dentition was segmented by adjusting the threshold range according to the image gray value and exported in STL file format. The STL files were imported into the reverse engineering software Geomagic Studio (version 2015; Geomagic, USA) to smooth the surface of the preliminary model through relaxation commands. Cortical bone, cancellous bone, and PDL were obtained through offset and Boolean commands and then were auto-surfaced to generate a NURBS curved parametric Computer - Aided Design (CAD) model (Fig. 1a). The uniform thickness of cortical bone and PDL was defined as 2.0 mm and 0.2 mm, respectively [20].

Four models were constructed and grouped as follows: Model A (fixed appliance), Model B (microimplant), Model C (clear aligner), and Model D (3D printed personalized device) (Fig. 1b). The 3D geometric models of brackets and archwire, microimplants, and 3D printed personalized device were generated by SolidWorks software (version 2016; Dassault, France). A rectangular archwire ($0.018 \times 0.025$ inch) was used to make two "T" loops at the mesial and distal side of the first molar to intrude it [21, 22]. To make the clear aligner in Model C, the first molar

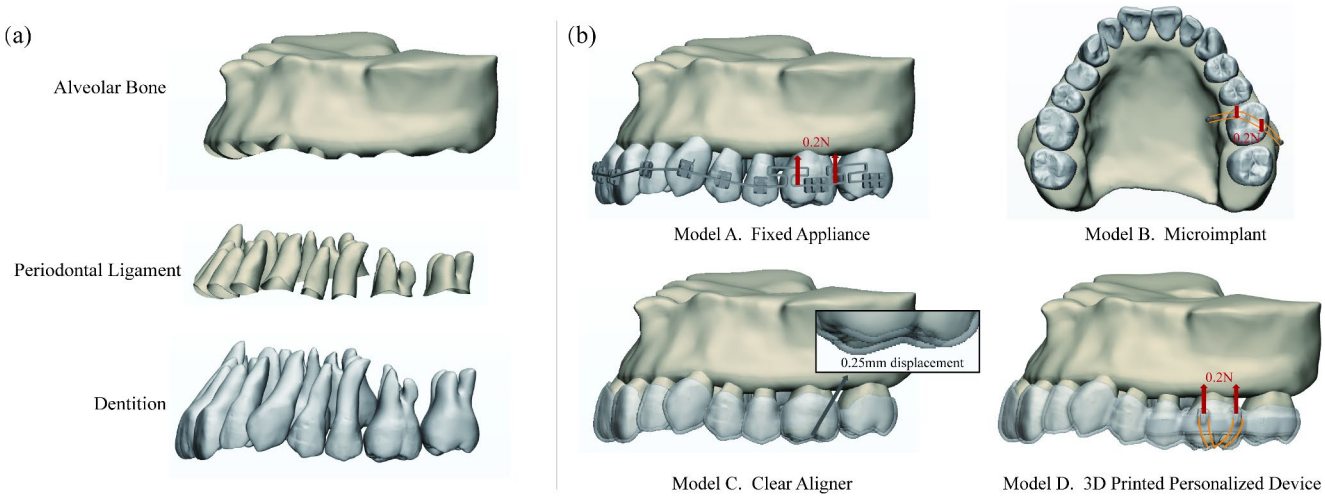


**Fig. 1** 3D geometric model design and grouping (**a**) Anatomic geometric model of alveolar bone, periodontal ligament and dentition. (**b**) Grouping of the four intrusion methods: Model (A) Fixed appliance; Model (B) Microimplant; Model (C) Clear aligner; Model (D) 3D printed personalized device

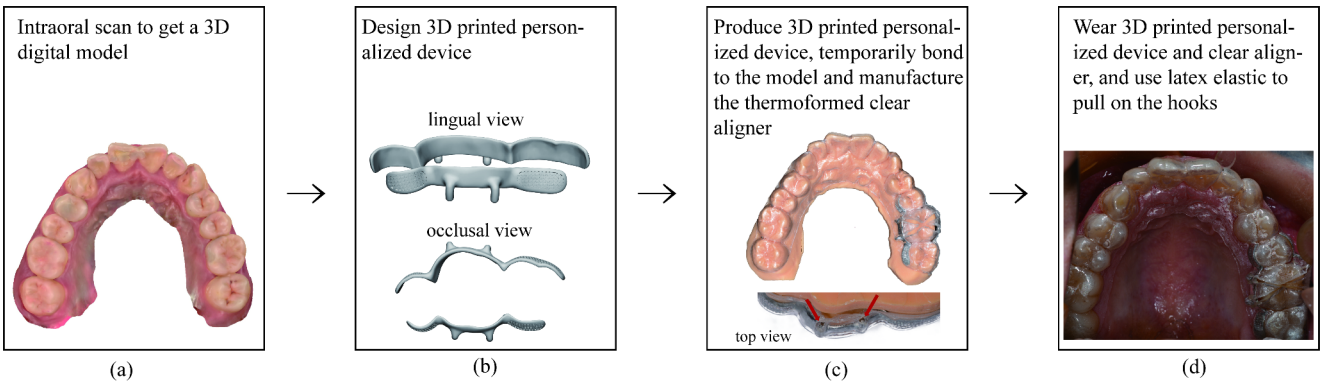


**Fig. 2** The process of manufacturing the 3D printed personalized device combined with the clear aligner in clinical practice

was intruded by 0.25 mm to get a new dentition, and then the crown surface of the dentition was cut along the gingival margin in the Geomagic software. The surface was uniformly offset outward by 0.7 mm [23] to generate a clear aligner. The clear aligner was then matched to the old dentition where the original first molar was not intruded, so that the intrusion amount of 0.25 mm [24] of the first molar was generated. The 3D printed personalized device was composed of the buccal and lingual bases that were fitted to the tooth surface. The second premolar and second molar were in contact with the bases, while the first molar was not in contact with them. Instead, four traction hooks were protruding toward the gingival direction on the buccal and lingual side for latex elastic traction (Fig. 2b). A clear aligner was created to wrap the auxiliary device and dentition, and an "X" shaped groove was created on the occlusal surface of the clear aligner to facilitate the application of the latex elastic on the target tooth (Fig. 2c).

## Properties and contact conditions

The models were assembled and imported into ABAQUS software (version 6.14; SIMULIA, France). Each subject was assumed to be a continuous homogeneous, isotropic linear elastic material [25]. The material properties of the components were shown in Table 1 [26, 27]. The modified 10-node tetrahedral element (C3D10M) was used to mesh the 3D model, and the approximate numbers of nodes and elements were shown in Table 1.

The top surface of the maxilla was completely constrained and no rotation or displacement in any direction occurred. Bonded connections were defined as the contact relationships between cortical and cancellous bone, maxilla and PDL, teeth and PDL, brackets and teeth, brackets and archwire, microimplants and maxilla, and 3D printed personalized device between teeth and clear aligner of model D. The contact relationship between the external surface of the crown and the inner surface of the clear aligner of model

**Table 1** Material properties and number of nodes and elements of the components of the finite element model

| Component | Young's modulus (MPa) | Poisson's ratio | Nodes | Elements |
|---|---|---|---|---|
| Teeth | 18,600 | 0.31 | 16,727–41,193 | 8913–22,424 |
| PDL | 0.68 | 0.48 | 23,742–71,950 | 11,922–36,913 |
| Cortical bone | 13,700 | 0.3 | 313,977–314,936 | 166,376–167,216 |
| Cancellous bone | 1370 | 0.3 | 151,732–153,377 | 81,633–83,063 |
| Clear aligner | 816.31 | 0.3 | 137,450–166,256 | 75,590–84,334 |
| *microimplant* | 112,000 | 0.33 | 67,570–69,682 | 44,972–46,322 |
| 3D printed device | 235,000 | 0.33 | 26,535–60,181 | 15,957–37,749 |
| Archwire | 200,000 | 0.3 | 10,740 | 5014 |
| Bracket | 210,000 | 0.3 | 4624–9495 | 2623–5770 |

C was defined as nonlinear face-to-face contact, and the coulomb friction coefficient was 0.2 [28]. A traction load of 0.2 N was applied on Model A, model B and model D [29].

The nonlinear iterative calculation of 3D model was carried out in the ABAQUS software, the calculative results were converged and the visualization results were output. The initial displacement of the maxillary teeth and the Von Mises stress distribution of the PDL were analyzed.

### Clinical application: manufacture of 3D printed personalized device combined with clear aligner

A pair of split springs were placed on the mesial and distal side of the first molar to obtain a gap to avoid obstruction during the intrusion. We designed the 3D printed personalized device based on the digital model formed by the intraoral scan of the dentition (Fig. 2a). And then the digital model was sent to denture manufacturing company (Chongqing Jingmei Denture Company) to get the 3D printed personalized device. The auxiliary device was consisted of buccal and lingual bases. The external surfaces were designed as grid plates to increase the contact stability between 3D printed personalized device and the clear aligner. The internal surfaces in contact with teeth were designed to be smooth, so that the patients could easily wear and remove the appliance (Fig. 2b). After 3D printed personalized device was printed with cobalt-chromium (Co-Cr) alloy, it was temporarily bonded to the plaster model, and the clear aligner was made by thermoplastic forming method to wrap the auxiliary device and dentition. Most part of the auxiliary device was wrapped by the clear aligner except the bottom part of hooks of the aligner. The bottom part is cut out to allow elastics to transmit force directly between the hooks (Fig. 2c). The clear aligner was precisely cut to form the "X" shaped traction groove for the target tooth intrusion. The latex elastics (1/4, 2oz, with a force about 30 g) were attached to the buccal and lingual traction hooks on 3D printed personalized device (Fig. 2d). The clear aligner and 3D printed personalized device could be removed for cleaning. After patients brush their teeth every night, the latex elastics should be replaced with new ones, and they were instructed to wear the clear aligner for at least 20 h a day.

## Results

### Comparison of initial displacements of target tooth

As shown in Fig. 3, among the four models, the comprehensive displacement trend of the target tooth in Model A, Model C, and Model D was similar, showing that the crown was mesially and buccally tipped, and the root was distally and lingually intruded, but the root of Model A was intruded lingually. In Model B, the crown of the target tooth showed distal and lingual tipping, and the root was buccally intruded. Among the four models, the clear aligner model had the maximum comprehensive displacement of the target tooth (55.98 μm), while the other three models showed little difference – the fixed appliance model (3.514 μm), 3D printed personalized device model (1.326 μm), and microimplant model (0.9976 μm). In the three-dimensional vector directions, the displacement in the buccolingual dimension of 3D printed personalized device model (7.429E-04 mm) was smaller than that of the fixed appliance model (3.078E-03 mm). The displacement in the mesiodistal dimension of 3D printed personalized device model (4.732E-04 mm) was smaller than that of the fixed appliance model (8.257E-04 mm). The displacement in the vertical dimension (1.134E-03 mm) was also smaller than that of the fixed appliance (2.226E-03 mm) (Fig. 4).

### Comparison of von mises stresses distribution in the PDL of target teeth

As shown in Fig. 5, in Model A, the stress in the PDL of the target tooth was concentrated on the distobuccal and lingual cervical margins. In Model B, the stress in the PDL of the target tooth was concentrated on the lingual and distal cervical margins and the root furcation area. In Model C, the stress in the PDL of the target tooth was mainly distributed in the mesial cervical margin. In Model D, the stress

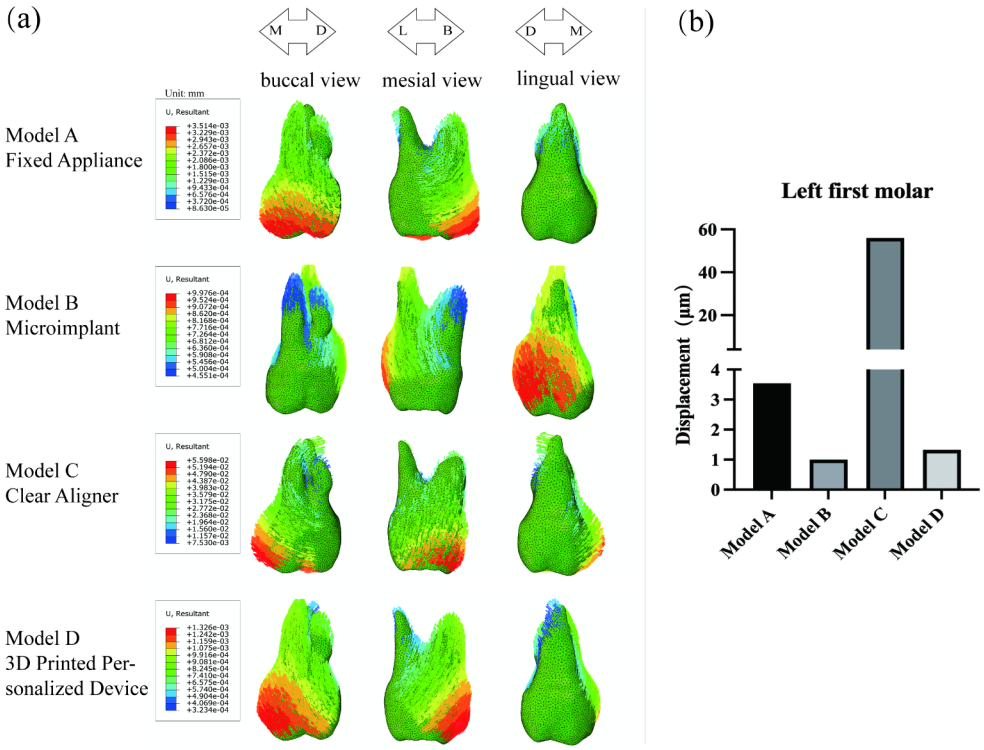


**Fig. 3** (**a**) The displacement tendencies of target tooth in four models. ("M" represents mesial direction, "D" represents distal direction, "L" represents lingual direction, "B" represents buccal direction). (**b**) The maximum resultant displacement of the target tooth in four models

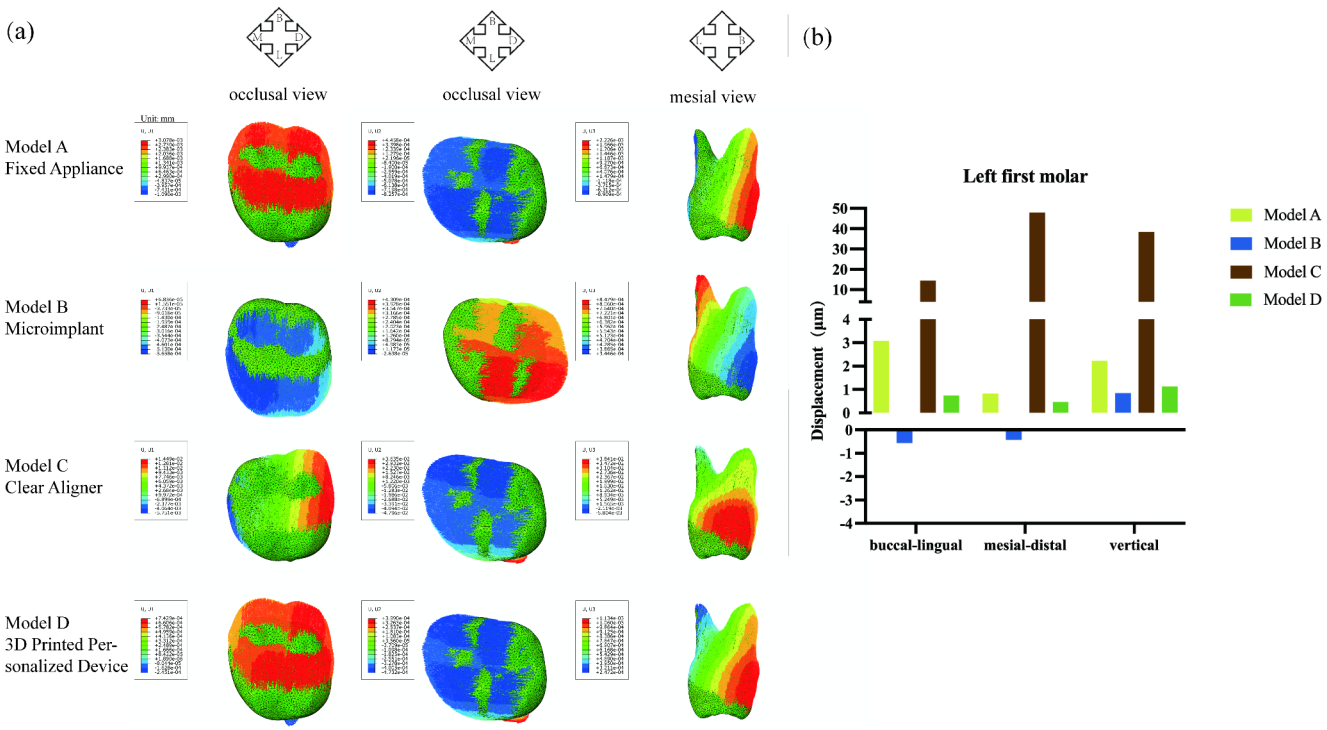


**Fig. 4** (**a**) The displacement pattern on target tooth in three dimensions including buccal-lingual direction, mesial-distal direction and vertical dimension. ("M" represents mesial direction, "D" represents distal direction, "L" represents lingual direction, "B" represents buccal direction). (**b**) The maximum displacement of the target tooth in three dimensions

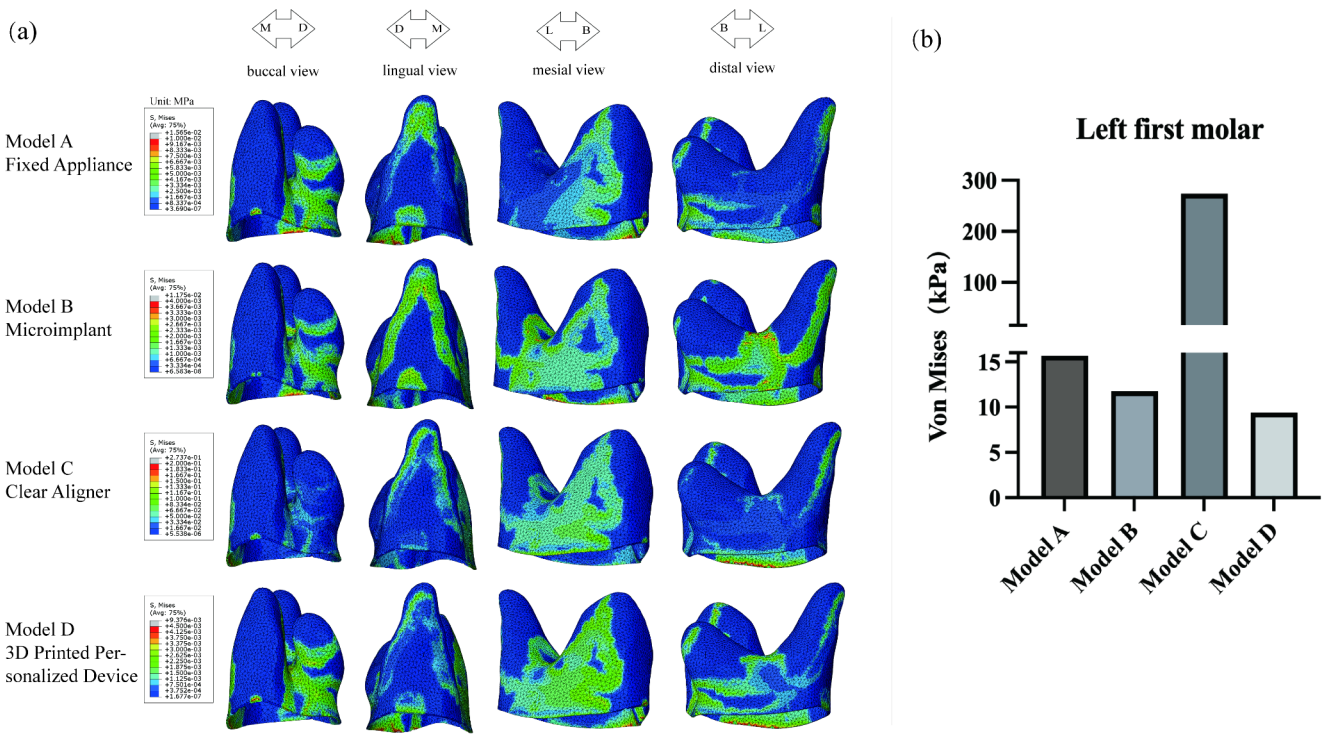


**Fig. 5** (**a**) The Von Mises stress distribution in the PDL of target tooth. ("M" represents mesial direction, "D" represents distal direction, "L" represents lingual direction, "B" represents buccal direction). (**b**) Stress value for average Von Mises in the PDL of target tooth

in the PDL was concentrated on the distobuccal and mesial cervical margins. Among the four models, the clear aligner model had the largest PDL stress (273.7 kPa), while the other three groups showed little difference – fixed appliance model (15.65 kPa), microimplant model (11.75 kPa), and 3D printed personalized device model (9.376 kPa).

## Comparison of the maximum comprehensive displacements of anchorage teeth

As shown in Fig. 6, the displacement tendencies of anchorage teeth in the four models were different. In Model A, the second premolar was buccally rotated, while the second molar was mesially and buccally rotated. In Model B, the second premolar was buccally tipped and the second molar was distally and lingually tipped. In Model C, the second premolar was lingually and distally extruded, and the second molar was lingually rotated. In Model D, the second premolar was lingually extruded, and the second molar was lingually and distally extruded. The maximum comprehensive displacement of the second premolar was observed in the clear aligner model (53.63 μm), followed by the fixed appliance model (0.7025 μm), 3D printed personalized device model (0.6551 μm), and the smallest in the microimplant model (0.01344 μm). The maximum comprehensive displacement of the second molar was observed in the clear aligner model (18.36 μm), followed by 3D printed personalized device model (0.6211 μm), the fixed appliance model (0.5605 μm), and the smallest in the microimplant anchorage model (0.01167 μm).

## Comparison of von mises stresses in the PDL of the anchorage teeth

As shown in Fig. 7, the stress distribution of second premolar in the four models showed little difference, and the major stress was concentrated on the apical area. In Model A, the stress in the PDL of the second molar was mainly concentrated on the mesial cervical margin. In Model B, the stress of the second molar was mainly concentrated on the distal cervical margin. In Model C and D, the stress of the second molar was mainly concentrated on the distobuccal cervical margin. The maximum stress value of second premolar was the clear aligner model (265.8 kPa), followed by 3D printed personalized device model (5.025 kPa), the fixed appliance model (2.261 kPa), and the microimplant model (0.04217 kPa). The maximum stress value of the second molar was the clear aligner model (81.64 kPa), followed by 3D printed personalized device model (3.496 kPa), the fixed appliance model (3.032 kPa), and the minimum in the microimplant model (0.07945 kPa).

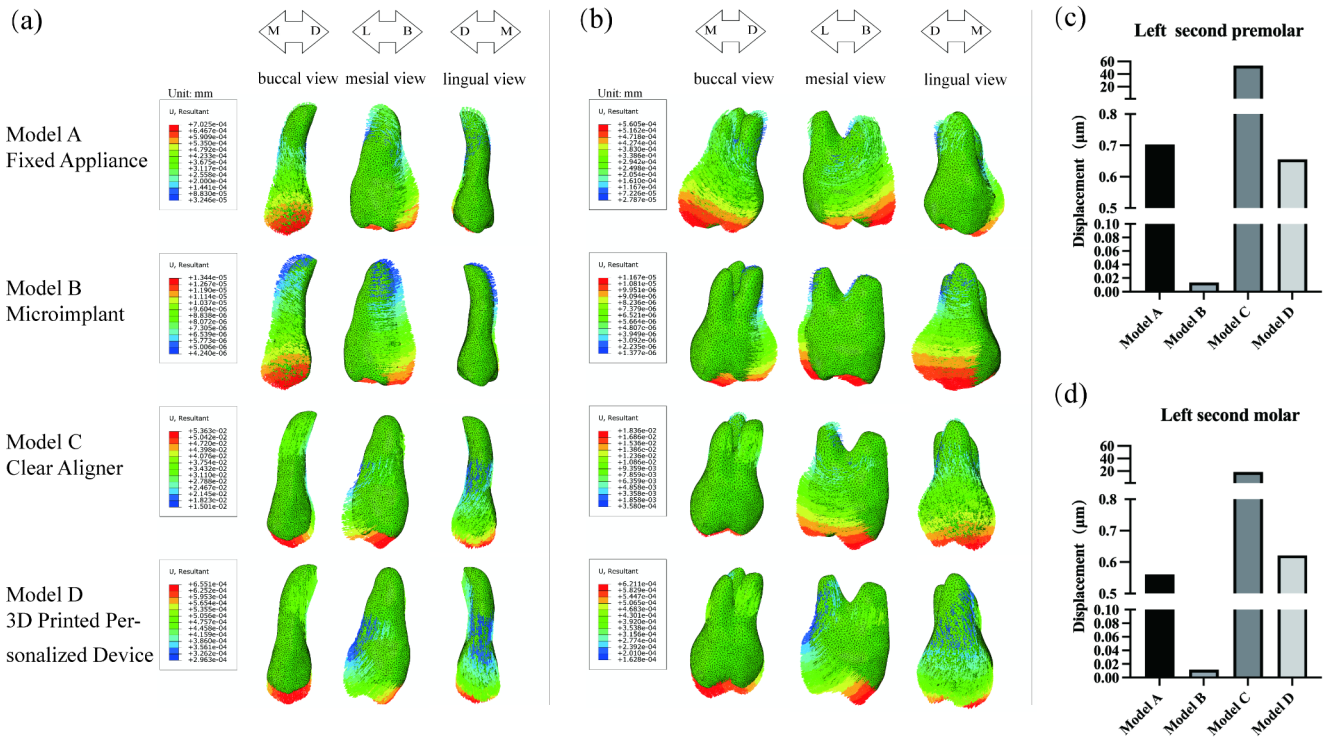


**Fig. 6** (**a**) The displacement tendencies of second premolar in four models. (**b**) The displacement tendencies of second molar in four models. ("M" represents mesial direction, "D" represents distal direction, "L" represents lingual direction, "B" represents buccal direction). (**c**) The maximum displacement of second premolar. (**d**) The maximum displacement of second molar

## Clinical application results

We applied 3D printed personalized device to the clinical case selected in this study (Fig. 8). After two months of treatment, the left first molar was successfully intruded, and the height of the marginal ridges of the adjacent teeth were the same as that of the marginal ridges of the first molar. The 3D overlap figure before and after treatment showed that the intrusion of the target tooth was about 1.5 mm, and a favorable treatment effect was obtained. Oral hygiene was well maintained after removing the appliance, and no dental caries or periodontitis occurred. The patient was satisfied with the treatment effect, including short time of treatment, simple treatment process and no discomfort with the appliance. A fixed retainer was made at the buccal and lingual surface of the second premolar, the first molar, and the second molar for retention.

## Discussion

This study aims to compare the biomechanical effect and intrusion effect of fixed appliance, microimplant, clear aligner, and 3D printed personalized device combined with clear aligner in the intrusion of the overerupted maxillary first molar. The results of the displacement tendency and the stress distribution in the PDL of the target tooth were different. The 3D printed personalized device model reflected its efficient intrusion on the target tooth and smaller stress concentration. For the anchorage teeth, the microimplant model showed advantages over the other three models.

In fixed appliance treatment, the intrusion loops of the archwire were created to generate the force for tooth movement, which not only has a vertical intrusion force but also has a buccal tipping effect when the overerupted molar is intruded [30]. The results of our study are consistent with this trend. Compared with the fixed appliance, the vertical displacement of the target tooth of 3D printed personalized device model was 50.94% (1.134E-03/2.226E-03) of the fixed appliance model. However, the buccal tipping effect was reduced by 75.86% [(3.078E-03-7.429E-04)/3.078E-03], and the mesial tipping effect was reduced by 42.7% [(8.257E-04-4.732E-04)/8.257E-04] compared with fixed appliance. For anchorage teeth, the second premolar and second molar of 3D printed personalized device model had smaller tipping displacement in the buccolingual and mesiodistal dimensions than those of the fixed appliance model, and there was little difference in the vertical displacement between the two models (Supplementary Fig. 1, 2). In terms of Von Mises stress of PDL, the stress of the target tooth of 3D printed personalized device model was lower than that of the fixed appliance model, but the

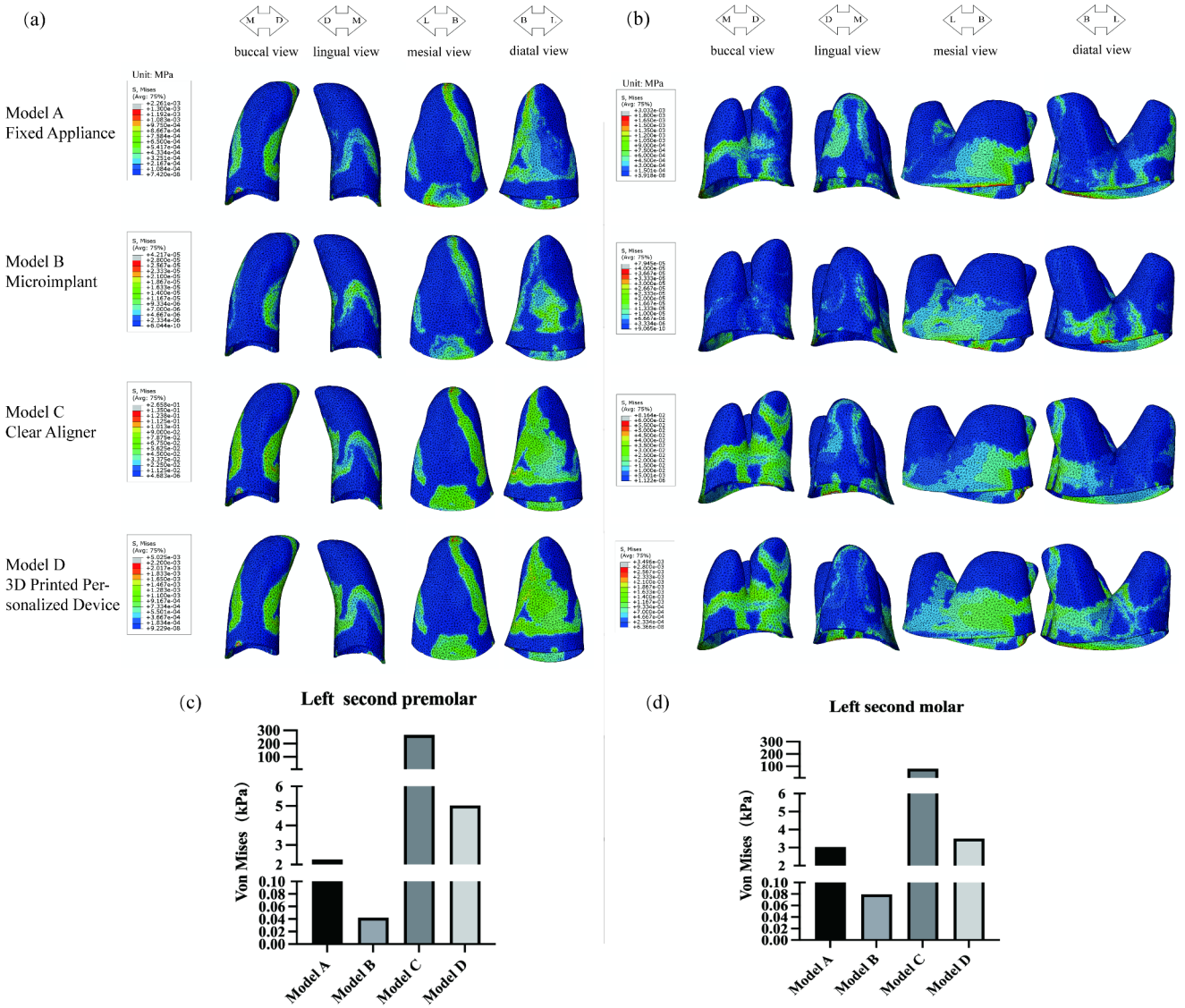


**Fig. 7** (**a**) The Von Mises stress distribution in the PDL of second premolar in four models. (**b**) The Von Mises stress distribution in the PDL of second molar in four models. ("M" represents mesial direction, "D" represents distal direction, "L" represents lingual direction, "B" represents buccal direction). (**c**) Stress value for average Von Mises in the PDL of second premolar. (**d**) Stress value for average Von Mises in the PDL of second molar

proportion of PDL stress of the anchorage teeth (31.42%) was higher than that of the fixed appliance model (21.66%) (Table 2). Compared with fixed appliance, 3D printed personalized device can achieve the intrusion effect of the target tooth while effectively reducing the adverse tipping effect of the target tooth and anchorage teeth. However, large stress concentration should be avoided in the design of anchorage teeth.

The microimplant model had the minimum intrusion value on the target tooth, which was about 75.23% (0.9976/1.326) of 3D printed personalized device model, while the stress on the PDL of the target tooth was about 1.25 (11.75/9.376) times of 3D printed personalized device model. However, compared with the other three models, the displacement and the stress distribution of PDL of adjacent teeth in the microimplant model were the minimum, which was almost negligible. This was the obvious advantage of the microimplant model compared with other methods [31]. Compared with the microimplant model, the use of 3D printed personalized device can obtain a better intrusion effect and less stress concentration effect of the target tooth, but it will produce a small amount of unfavorable displacement and stress distribution of adjacent teeth.

The displacement and Von Mises stress of the PDL of other teeth in fixed appliance model, microimplant model and 3D printed personalized device model were

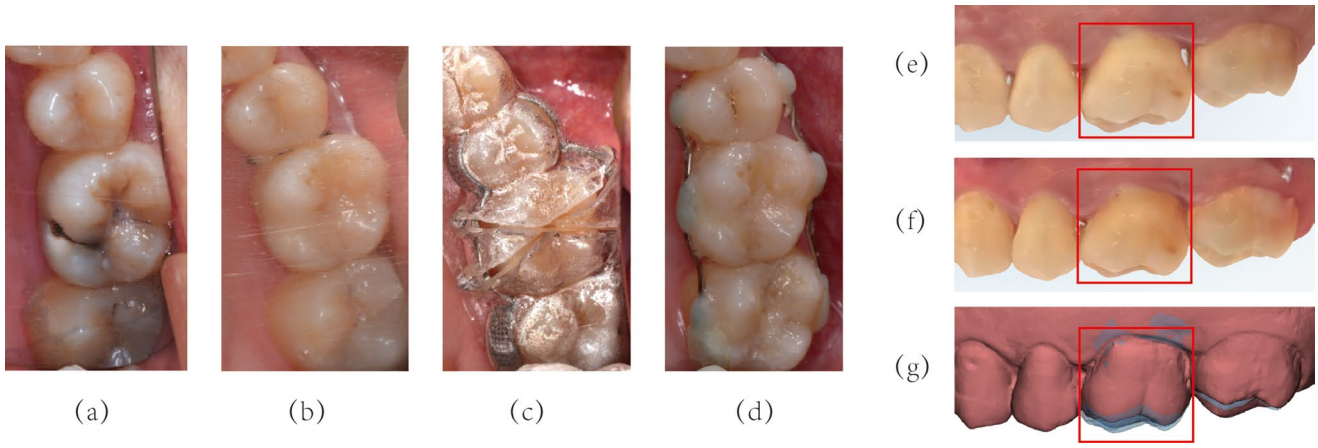


**Fig. 8** The treatment results of the clinical case. (**a**) The intraoral picture of overerupted first molar before treatment. (**b**) Use of a pair of split springs to obtain gaps before intrusion. (**c**) The 3D printed personalized device combined with clear aligner was wore on the dentition and latex elastic was used to load force. (**d**) The first molar was successfully intruded and a fixed retainer was made at the buccal and lingual surface of the second premolar, the first molar, and the second molar for retention. (**e**) Intraoral scan of the overerupted first molar before treatment. (**f**) Intraoral scan of the overerupted first molar after treatment. (**g**) The 3D overlap figure before and after treatment of the intrusion effect

similar (Supplementary Fig. 3, 4), and all showed a gradually decreasing trend from the adjacent teeth to the distal dentition, while the trend of the clear aligner model was different. A large displacement and significant PDL stress were observed at the left central incisor, the right lateral incisor, the left first premolar, and the left lateral incisor in the clear aligner model which showed obvious force on the anterior teeth (Table 2). Because the teeth were not aligned in our study, the rotation of the incisors may lead to greater displacement tendency due to the stress concentration effect. Besides, the anterior teeth were mostly single root, and the alveolar bone was thin there. However, this phenomenon did not occur in Model D because of the different force application methods that it used auxiliary device to provide force application instead of clear aligner. The use of 3D printed personalized device is beneficial to reduce the stress concentration on the anterior teeth, thereby reducing the risk of root and alveolar bone resorption, which is similar to the results of Jia's study [32].

The intrusion of the target tooth, anchorage teeth and the stress of PDL in the clear aligner model were significantly greater than those of the other three groups. One reason may be that a small force of 20 g was applied on the fixed appliance model, microimplant model, and 3D printed personalized device model. The displacement and stress values of the PDL were small under this light force. In the process of tooth intrusion, the force was often concentrated on the apical region, and the intrusion was often more likely to cause root resorption than other types of tooth movement. Akl et al. and Al-Falahi et al. also found that root resorption occurred in the process of posterior tooth intrusion [33, 34]. Force between 10 and 20 g is often recommended for teeth intrusion [29]. Since the intrusion of a single molar does not require much force, we did not design retention attachments. However, in the case of multiple molars or large displacement of intrusion, designing retention attachments on adjacent teeth or bonding 3D printed device to the tooth surface may be necessary. Whether this force is the best for various intruding methods needs further experimental investigation. The second reason was that clear aligner was made of elastic materials, which were prone to deformation due to insufficient stiffness [35, 36]. In the clear aligner group, the target tooth was designed with 0.25 mm displacement interference intrusion. Stress relaxation tests of clear aligner show the maximum initial stress when the load is first applied, with stress reducing by more than 50% within 24 h [37]. It is unclear how much intrusion displacement and stress can be produced by this method, which needs to be verified by further research. Compared with the other three groups, provided with continuous light force, the actual intrusion effect still needs to be confirmed by more complete clinical research.

For clinical application, this patient lost his left mandibular first molar and the opposing tooth was overerupted. The patient refused comprehensive orthodontic treatment. Thus, the intrusion of the overerupted tooth was a preparation for prosthetic treatment and did not contain the movement of the rest of the dentition. Based on the patient's willingness not to accept invasive operation and bad oral hygiene, we applied 3D printed personalized device combined with clear aligner to clinical practice (Fig. 8). During the whole process of orthodontic treatment, we only used one single clear aligner as a container of the 3D printed personalized device. The 3D printed personalized device and the dentition were wrapped by the clear aligner,

**Table 2** Von mises stress (kPa) on PDL of all teeth and corresponding percentages in different intrusion models used

| Model | 17 | 16 | 15 | 14 | 13 | 12 | 11 | 21 | 22 | 23 | 24 | 25 | 26 | 27 | TOTAL |
|---|---|---|---|---|---|---|---|---|---|---|---|---|---|---|---|
| A | 1.63E-07 | 3.69E-02 | 2.06E-02 | 2.10E-02 | 0.0502 | 8.55E-02 | 0.1298 | 0.199 | 0.2755 | 0.7499 | 1.93 | 2.261 | 15.65 | 3.032 | 2.44E+01 |
| | 0.00% | 0.15% | 0.08% | 0.09% | 0.21% | 0.35% | 0.53% | 0.81% | 1.13% | 3.07% | 7.90% | 9.25% | 64.03% | 12.41% | |
| B | 1.79E-05 | 8.32E-05 | 1.82E-04 | 3.62E-04 | 6.69E-04 | 9.69E-04 | 6.45E-04 | 1.84E-03 | 9.59E-04 | 4.99E-03 | 1.41E-02 | 4.22E-02 | 11.75 | 7.95E-02 | 1.19E+01 |
| | 0.00% | 0.00% | 0.00% | 0.00% | 0.01% | 0.01% | 0.01% | 0.02% | 0.01% | 0.04% | 0.12% | 0.35% | 98.77% | 0.67% | |
| C | 4.179 | 47.2 | 16.97 | 69.91 | 121 | 105.3 | 53.45 | 131 | 52.03 | 36.07 | 130.1 | 265.8 | 273.7 | 81.64 | 1388.349 |
| | 0.30% | 3.40% | 1.22% | 5.04% | 8.72% | 7.58% | 3.85% | 9.44% | 3.75% | 2.60% | 9.37% | 19.15% | 19.71% | 5.88% | |
| D | 5.99E-02 | 0.1138 | 0.2282 | 0.2169 | 0.4276 | 0.3861 | 0.6237 | 0.5965 | 0.8329 | 1.663 | 4.078 | 5.025 | 9.376 | 3.496 | 2.71E+01 |
| | 0.22% | 0.42% | 0.84% | 0.80% | 1.58% | 1.42% | 2.30% | 2.20% | 3.07% | 6.13% | 15.03% | 18.53% | 34.57% | 12.89% | |

which was beneficial for retention and force transmission. In addition, the auxiliary device is not bonded to tooth surface and could be removed for cleaning, which is beneficial to maintain good oral hygiene. And for patients with prosthetic crowns that are not suitable for appliance bonded to tooth surface, this 3D printed personalized device combined with clear aligner could provide a treatment possibility. However, for cases where excessive tooth overeruption leads to a very narrow gap, this method may not be as effective as clear aligners or microimplants. The integration of 3D printed clear aligners and metal auxiliary devices may solve this issue in the future. Attention should be paid to strengthening the anchorage control of adjacent teeth to reduce the adverse effects for further optimization.

The finite element analysis has certain limitations which only describe the initial effect of tooth displacement and stress of PDL under the intruding force, and cannot simulate the displacement trend under long-term orthodontic treatment, such as in clinical practice. Besides, the property of PDL was assumed to be a linear elastic material in our study, that has some distinction from its non-linear behavior in vivo. However, study shows that there is no significant difference in mechanical response of PDL between linear and non-linear model when the tooth displacement is small [38]. Moreover, the occlusal forces were not incorporated into the analysis. The occlusal force could partially counteract this extrusion force on the anchorage teeth and the dislodging forces on the clear aligner. In addition, although personalized devices have shown an exact effect in clinical application, the actual comparison among the four models has not been carried out. Whether it is the best method of force application needs to be verified by a certain amount of clinical cases and related researches.

## Conclusion

All four patterns could achieve molar intrusion. The 3D printed personalized device had relatively higher intrusion efficiency and lower stress distribution on the target tooth, and reduced the displacement and stress concentration of the anchorage teeth to a certain extent. In clinical practice, 3D printed personalized device has achieved good therapeutic results.

**Supplementary Information** The online version contains supplementary material available at https://doi.org/10.1007/s00784-025-06327-z.

**Acknowledgements** Not applicable.

**Author contributions** QX contributed to: validation, methodology, formal analysis, data curation, investigation, Writing - Original Draft. MH contributed to: methodology, supervision. MLX contributed to: methodology, supervision. XYZ contributed to: methodology, supervision. HQW contributed to: methodology, supervision. MMS contributed to: methodology, supervision. CJW contributed to: conceptualization, validation, methodology, software, Writing - Review and Editing.

YH contributed to: conceptualization, funding acquisition, methodology, Writing - Review and Editing.

**Funding** This work was supported by 2024 Chongqing Young and middle-aged medical Talents Project (YXGD202438), Chongqing medical scientific research project (Joint project of Chongqing Health Commission and Science and Technology Bureau: 2024MSXM070), Chinese Stomatological Association Youth Clinical Research Foundation for Orthodontics (CSAO2020- 07), Stomatological Hospital of Chongqing Medical University (Program: The 3D printed device assisted local orthodontic treatment before the restoration of posterior teeth), Chongqing medical scientific research project (Joint project of Chongqing Health Commission and Science and Technology Bureau: 2024QNXM013).

**Data availability** No datasets were generated or analysed during the current study.

## Declarations

**Ethics approval and consent to participate** This study was approved by the ethics committee of the Stomatological Hospital of Chongqing Medical University and the ethics number is (2020)094. Informed consent to participate was obtained from all of the participants in the study.

**Competing interests** The authors declare no competing interests.



## References

1. Lee BA, Kim B, Kim YT (2020) Supraeruption as a consideration for implant restoration. J Periodontal Implant Sci 50(4):260–267
2. Rai D, Bhasin SS, Rai S (2014) Orthodontic microimplants assisted intrusion of Supra-erupted maxillary molar enabling osseointegrated implant supported mandibular prosthesis: case reports. J Indian Prosthodont Soc 14(Suppl 1):238–242
3. Arsenina OI, Abakarov SI, Popova NV, Makhortova PI, Popova AV, Zhukov DY (2023) Orthodontic treatment as a stage of rational dental prosthetics. Stomatologiia (Sofiia) 102(2):54–62
4. Marya A, Winoto ER (2023) Adjunctive controlled intrusion of the maxillary first molar using orthodontic miniscrews. J Surg Case Rep 2023(2):1–3
5. Sohn DS, Lee JK, An KM (2008) Minor tooth movements using microimplant Anchorage: case reports. Implant Dent 17(1):32–39
6. Sivakumar I, Sivakumar A (2014) Intrusion of an overerupted molar using orthodontic Miniscrew implant: A preprosthodontic therapy. Contemp Clin Dent 5(3):422–424
7. Yang Y, Yang R, Liu L et al (2023) The effects of aligner anchorage Preparation on mandibular first molars during premolar-extraction space closure with clear aligners: A finite element study. Am J Orthod Dentofac Orthop 164(2):226–238
8. Muro MP, Caracciolo ACA, Patel MP, Feres MFN, Roscoe MG (2023) Effectiveness and predictability of treatment with clear orthodontic aligners: A scoping review. Int Orthod 21(2):100755
9. Kravitz ND, Kusnoto B, BeGole E, Obrez A, Agran B (2009) How well does invisalign work? A prospective clinical study evaluating the efficacy of tooth movement with invisalign. Am J Orthod Dentofac Orthop 135(1):27–35
10. Tartaglia GM, Mapelli A, Maspero C et al (2021) Direct 3D printing of clear orthodontic aligners: current state and future possibilities. Materials 14(7):1799
11. Ratzmann A, Weßling M, Krey KF (2023) Design, numerical simulation and in vitro examination of a CAD/CAM fabricated active orthodontic treatment element. Int J Comput Dent 26(2):125–136
12. Nguyen VA (2024) 3D-printed indirect bonding trays and transfer jigs for lingual brackets: digital workflows and two case reports. Heliyon 10(11):e32035
13. Nguyen VA, Nguyen TA (2023) Digital workflows for 3D-printed customised double-slotted lingual appliances: a case report. Aust Orthod J 39:100–112
14. Çifter M, Saraç M (2011) Maxillary posterior intrusion mechanics with mini-implant anchorage evaluated with the finite element method. Am J Orthod Dentofac Orthop 140(5):233–241
15. Zhang Y, Zheng X, Zhang Q et al (2023) Clinical finite element analysis of mandibular displacement model treated with Twin-block appliance. Am J Orthod Dentofac Orthop 164(3):395–405
16. Sugii MM, Barreto B, de Vieira-Júnior CFF, Simone W, Bacchi KRI, Caldas A RA (2018) Extruded upper first molar intrusion: comparison between unilateral and bilateral Miniscrew anchorage. Dent Press J Orthod 23(1):63–70
17. Fan D, Liu H, Yuan CY, Wang SY, Wang PL (2022) Effectiveness of the attachment position in molar intrusion with clear aligners: a finite element study. BMC Oral Health 22(1):474
18. Zhang JF, Hu YC, Wang BC, Wang L, Wang H, Li Y, Yan M, Liu HT (2020) 3D finite element analysis of the modular prosthesis with tooth mechanism of the femoral shaft. Orthop Surg 12(3):946–956
19. Katta M, Petrescu SMS, Dragomir LP et al (2023) Using the finite element method to determine the Odonto-Periodontal stress for a patient with angle class II division 1 malocclusion. Diagnostics 13(9):1567
20. Kim WH, Hong K, Lim D, Lee JH, Jung YJ, Kim B (2020) Optimal position of attachment for removable thermoplastic aligner on the lower canine using finite element analysis. Mater (Basel) 13(15):3369
21. Bi S, Guo Z, Zhang X, Shi G (2022) Anchorage effects of ligation and direct occlusion in orthodontics: A finite element analysis. Comput Methods Programs Biomed 226:107142
22. Haris TPM, Francis PG, Margaret VA, Roshan G, Menon V, Jojee V (2018) Evaluation of Biomechanical properties of four loops at different activation: A finite element method study. J Contemp Dent Pract 19(7):778–784
23. Mao B, Tian Y, Xiao Y, Li J, Zhou Y (2023) The effect of maxillary molar distalization with clear aligner: a 4D finite-element study with staging simulation. Prog Orthod 15(1):16
24. Zhang Y, Gao J, Wang X et al (2023) Biomechanical factors in the open gingival embrasure region during the intrusion of mandibular incisors: A new model through finite element analysis. Front Bioeng Biotechnol 11:1149472

25. Zeno KG, Mustapha S, Ayoub G, Ghafari J (2020) Effect of force direction and tooth angulation during traction of palatally impacted canines: A finite element analysis. Am J Orthod Dentofac Orthop 157(3):377–384
26. Xia Q, He Y, Jia L et al (2022) Assessment of labially impacted canines traction mode with clear aligners vs. fixed appliance: A comparative study based on 3D finite element analysis. Front Bioeng Biotechnol 10:1004223
27. Zhang WT, Cheng KJ, Liu YF, Wang R, Chen YF, Ding YD, Yang F, Wang LH (2022) Effect of the prosthetic index on stress distribution in Morse taper connection implant system and peri-implant bone: a 3D finite element analysis. BMC Oral Health 22(1):431
28. Jiang T, Wu RY, Wang JK, Wang HH, Tang GH (2020) Clear aligners for maxillary anterior En masse Retraction: a 3D finite element study. Sci Rep 10(1):10156
29. Proffit WR, Fields HW, Sarver DM (2013) Contemporary orthodontics[M], 5th edn. Elsevier
30. Martins RP, Shintcovsk RL, Shintcovsk LK, Viecilli R, Martins LP (2018) Second molar intrusion: continuous arch or loop mechanics? Am J Orthod Dentofac Orthop 154(5):629–638
31. Baumgaertel S, Smuthkochorn S, Palomo JM (2016) Intrusion method for a single overerupted maxillary molar using only palatal mini-implants and partial fixed appliances. Am J Orthod Dentofac Orthop 149(3):411–415
32. Jia L, Wang C, Li L et al (2023) The effects of lingual buttons, precision cuts, and patient-specific attachments during maxillary molar distalization with clear aligners: comparison of finite element analysis. Am J Orthod Dentofac Orthop 163(1):e1–e12
33. Akl HE, El-Beialy AR, El-Ghafour MA, Abouelezz AM, El Sharaby FA (2021) Root resorption associated with maxillary buccal segment intrusion using variable force magnitudes. Angle Orthod 91(6):733–742
34. Al-Falahi B, Hafez AM, Fouda M (2018) Three-dimensional assessment of external apical root resorption after maxillary posterior teeth intrusion with miniscrews in anterior open bite patients. Dent Press J Orthod 23(6):56–63
35. Liu J, qi, Zhu G, yin, Wang Y gan, Zhang B, Yao K, Zhao Z (2023) he Different biomechanical effects of clear aligners in closing maxillary and mandibular extraction spaces: Finite element analysis. Am J Orthod Dentofacial Orthop 163(6):811–824
36. Mao B, Tian Y, Li J, Zhou Y (2023) Expansion rebound deformation of clear aligners and its Biomechanical influence: a three-dimensional morphologic analysis and finite element analysis study. Angle Orthod 93(5):572–579
37. Lombardo L, Martines E, Mazzanti V, Arreghini A, Mollica F, Siciliani G (2016) Stress relaxation properties of four orthodontic aligner materials: A 24-hour in vitro study. Angle Orthod 87(1):11–18
38. Wu J, Liu Y, Li B, Dong X (2022) Development and verification of a constitutive model for human periodontal ligament based on finite element analysis. Comput Methods Biomech Biomed Engin 25(9):1051–1062